Control of robot-assisted gait trainer using hybrid proportional integral derivative and iterative learning control

Elang Parikesit[1], Dechrit Maneetham[1], Petrus Sutyasadi[2]
[1]Department of Mechatronics Engineering, Rajamangala University of Technology Thanyaburi, Thailand
[2]Mechatronics Department, Faculty of Vocational, Sanata Dharma University, Yogyakarta, Indonesia

Article Info

ABSTRACT

An inexpensive exoskeleton of the lower limb was designed and developed in this study. It can be used as a gait trainer for persons with lower limb problems. It plays an essential role in lower limb rehabilitation and aid for patients, and it can help them improve their physical condition. This paper proposes a hybrid controller for regulating the lower limb exoskeleton of a robot-assisted gait trainer that uses a proportional integral and derivative (PID) controller combined with an iterative learning controller (ILC). The direct current motors at the hip and knee joints are controlled by a microcontroller that uses a preset pattern for the trajectories. It can learn how to monitor a trajectory. If the trajectory or load is changed, it will be able to follow the change. The experiment showed that the PID controller had the smallest overshoot, and settling time, and was responsible for system stability. Even if there are occasional interruptions, the tracking performance improves with the ILC.

Corresponding Author:

Dechrit Maneetham
Department of Mechatronics Engineering, Rajamangala University of Technology Thanyaburi
Tambon Khlong Hok, Amphoe Khlong Luang, Pathum Thani, Thailand
Email: dechrit_m@rmutt.ac.th

1. INTRODUCTION

The term "cardiovascular disease" refers to a collection of illnesses that include heart disease, brain vascular disease, and diseases of other blood arteries. A kind of cardiovascular disease (CVD) is stroke [1]. Stroke ranks number 5 among all causes of death and the second-leading cause of death behind ischemic heart disease [2]. Neurological injuries, such as strokes and spinal cord injuries, often cause physical ailments that affect a person's ability to walk stroke is a significant disease in Asia, where more than 60% of the world's population lives. Except for a few nations like Japan, stroke deaths are higher in Asia than in Western Europe, America, or Australia [3]. Loss of walking ability often leads to dependence on wheelchairs or other mobility aids such as orthoses. Restoring the ability to walk is one of the main goals of recovery for many with neurological disorders. Various treatments have been used to re-learn motor skills and performance of walking by using robotic devices [4], [5]. There are walking trainers using robots available in the market, but the price is still very high [6]. Frugal Innovation is described as the potential to "do more with less"-that is, to generate considerably more market and social benefit while reducing the use of finite resources like electricity, money, and time [7]. In resource-constrained settings, healthcare providers often devise novel approaches to deliver sufficient treatment to patients. These low-cost yet practical, frugal inventions may have flaws, but they have the potential to make wellness more accessible to everyone [8].

With its high reliability and ease of implementation, proportional integral and derivative (PID) is the most often used controller because of its great dependability and simplicity of installation. However, a

PID-only controller is unsuitable for an exoskeleton robot due to variables such as variations in load, friction, and external interference [9], [10]. On the other hand, there is an iterative learning control algorithm (ILC) that, even though it is excellent at controlling repeated motions, has a significant tracking error and an unclear initial value, making it difficult to use in practice [11], [12]. There are some ideas of using a hybrid controller such as PID-ILC in improving the trajectory of a mechanism [13], but it was never implemented in the lower limb exoskeleton. Majeed *et al.* [14] already used the other types of hybrid controller, proportional derivative (PD) with particle swarm optimization (PSO), for the lower limb exoskeleton. It has better joint tracking performance, but upon the presence of disturbance, its efficacy deteriorates. Meanwhile, Amiri *et al.* [15] used PID with model reference adaptive control (MRAC). The speed and performance are better than PID, but there is an overshoot and gradually returns to the desired position. The goal of this research is to optimize the robot-assisted walking trainer's lower limb exoskeleton's control algorithm by utilizing hybrid PID-ILC to track the reference trajectory even when the lower limb is under varied load (disturbance) without going overshoot.

2. METHOD

2.1. System design

As shown in Figure 1, the fundamental control strategies of robot-assisted gait trainers were covered within a three-level framework that corresponds to the structure and functionality of the human neurological system. Being able to work together or separately, these levels are independent of each other [16]. This research robot of a robot-assisted gait trainer deals with the low level of control.
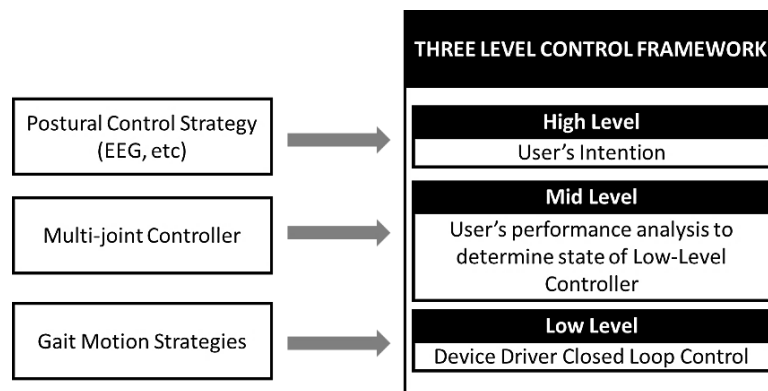

Figure 1. Hierarchical control framework of robot-assisted gait trainer

2.2. The kinematics for lower limb exoskeleton

The lower link exoskeleton is a two-link planar revolute-revolute arm. Figure 2 [17] shows such a 2 revolute (2R) planar manipulator with two revolute-revolute links. The inverse kinematics of a lower limb exoskeleton is similar to that of a planar robot in that it is easier to discover analytically. The tip point's global location is shown in (1).

$$\begin{bmatrix} X \\ Y \end{bmatrix} = \begin{bmatrix} l_1 \sin\theta_1 + l_2 \sin(\theta_1 + \theta_2) \\ l_1 \cos\theta_1 + l_2 \cos(\theta_1 + \theta_2) \end{bmatrix} \tag{1}$$

Therefore:

$$X^2 + Y^2 = l_1^2 + l_2^2 + 2l_1 l_2 \cos\theta_2 \tag{2}$$

and:

$$\cos\theta_2 = \frac{X^2 + Y^2 - l_1^2 - l_2^2}{2l_1 l_2} \tag{3}$$

$$\theta_2 = \cos^{-1}\frac{X^2 + Y^2 - l_1^2 - l_2^2}{2l_1 l_2} \tag{4}$$

Due to their inaccuracy, Arcsin and Arccos are typically avoided. As a result, we use the half-angle formula.

$$tan^2 \frac{\theta}{2} = \frac{1-\cos\theta}{1+\cos\theta} \tag{5}$$

To find θ_2 using an arctan 2 function:

$$\theta_2 = \pm arctan1 \sqrt{\frac{(l_1+l_2)^2-(X^2+Y^2)}{(X^2+Y^2)-(l_1+l_2)^2}} \tag{6}$$

Square root generates two solutions. Thus, the sign $\pm$ is needed. Based on geometry, the initial joint variable configuration may be determined as (7):

$$\theta_1 = arctan\, 2 \frac{Y}{X} + arctan\, 2 \frac{l_2 \sin\theta_2}{l_1+l_2 \cos\theta_2} \tag{7}$$

The following alternate equation can also be used:

$$\theta_1 = arctan\, 2 \frac{-Xl_2 \sin\theta_2 + Y(l_1+l_2 \cos\theta_2)}{Yl_2 \sin\theta_2 + X(l_1+l_2 \cos\theta_2)} \tag{8}$$

when X has a positive or negative sign, the value of θ_1 should be changed by adding or removing π. In addition, the equations can be concatenated as (9).

$$\begin{bmatrix} X \\ Y \end{bmatrix} = \begin{bmatrix} l_1 \sin\theta_1 + l_2 \sin(\theta_1 + \theta_2) \\ l_1 \cos\theta_1 + l_2 \cos(\theta_1 + \theta_2) \end{bmatrix} \tag{9}$$

Therefore, to determine a trigonometric equation for θ_1:

$$2Xl_1 \cos\theta_1 + 2Yl_1 \sin\theta_1 = X^2 + Y^2 + l_1^2 - l_2^2 \tag{10}$$

Additionally, the (11) can be used:

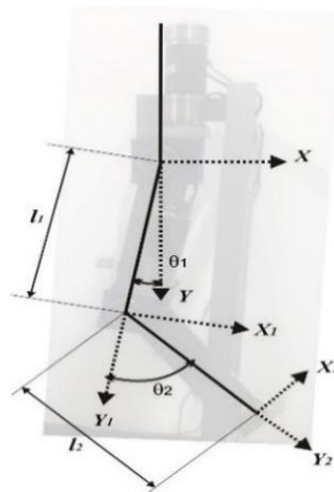$$l_1 + l_2 \cos\theta_2 = \frac{X^2+Y^2+l_1^2-l_2^2}{2l_1} \tag{11}$$

Figure 2. Lower limb exoskeleton kinematics

2.3. Mechanical design
There is a similarity between the human and the produced robotic joint for the knee as shown in Figures 3(a) and 3(b). Flexion and extension and internal and external rotation of a knee are shown in

Figure 3(a) [18]. While the knee part of the exoskeleton of the gait trainer is shown in Figure 3(b). The exoskeleton being developed only uses the sagittal plane as the range of motion (flexion and extension). To protect the user from injury, the range of joint angles is mechanically limited. Table 1 displays the values of hip and knee kinematics [19].
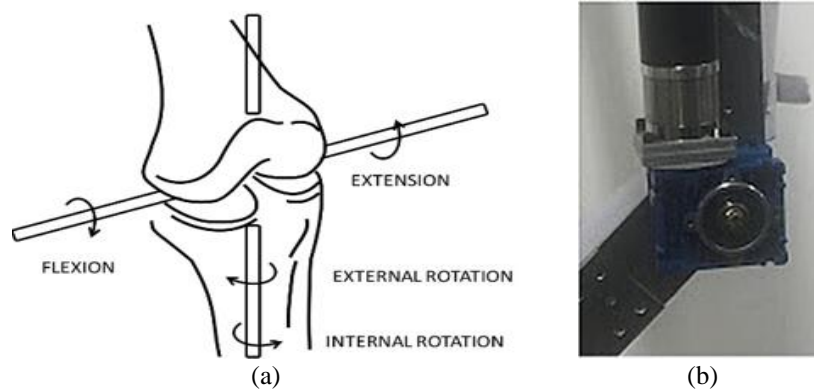

(a)   (b)

Figure 3. Comparison of (a) the human knee joint compared with (b) the exoskeleton joint

Table 1. Kinematics of hip and knee

	Motion	Range of Motion (degree)	Average Torque (Nm)
Hip	Flexion	100-140	140
	Extension	15-30	120
Knee	Flexion	120-140	140
	Extension	0-10	15

The exoskeleton is made to be as light as possible. It is envisioned as a four-degrees of freedom (DoF) bilateral wearable device with actuators at the joints of the hip and knee. The mechanical drawing of the lower limb exoskeleton can be seen in Figure 4. Aluminum is used in the mechanical structure to accommodate mechanical resistance and reduce weight [20].
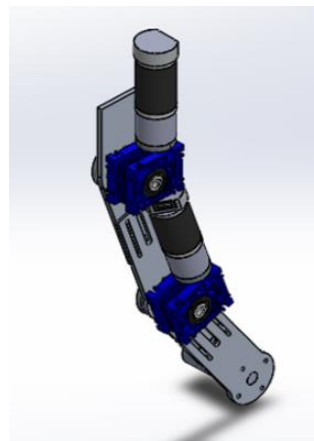

Figure 4. Mechanical drawing of lower limb exoskeleton

The movement equipment was selected according to each joint's tension and force values when walking at a typical speed. Direct current (DC) motors meet the performance criteria for a portable device's small solution. Because exoskeleton joints demand higher torque and lower speeds, DC motors can be connected directly to the gearbox to boost torque and reduce speed [21]. As shown in Figure 5(a) PG56 encoder brushed DC motor is used as the actuator, while Figure 5(b) shows the gearbox that is connected to

DC motor to increase the torque by 50 times. As shown in Figure 6, there are four DC motors to drive four joints in this lower limb exoskeleton), two motors for the left side, and two motors for the right side. The DC servo motors control the joint motors (PG56) using pulse width modulation (PWM) outputs from the microcontroller.

| (a) | (b) |

Figure 5. The actuator consists of (a) a PG56 encoder brushed DC motor that is connected to (b) a gearbox with shaft ratio 1:50

Figure 6. Lower limb exoskeleton with hip and knee joints

2.4. PID control

The first PID controller was ship autopilot owned by Elmer Sperry in 1910. Since Ziegler and Nichols [22] developed the methods of PID tuning in 1942, the popularity of the controller has risen even more [23]. Changes are required for three parameters in PID control [24]: the proportional, integral, and derivative. However, the PID control parameter adjustment affects system performance, such as stability and robustness [25]. Classical control theory provides a strong set of study tools to analyze closed-loop systems and build feedback controllers. The reference variable is sometimes referred to as the set point. The PID gain is the sum of the P-term, the I-term, and the D-term. A control action also can be viewed as a combination of integral, proportional, and derivative parts of a mathematical expression. The PID algorithm may be summarized as (12):

$$u(t) = K \left(e(t) + \frac{1}{T_i} \int_0^t e(\tau) d\tau + T_d \frac{de(t)}{dt} \right) \tag{12}$$

where y is measured process variable, r is reference variable, u is control signal, e is control error $(e = y_{sp} - y)$, K is proportional gain, T_i is integral time, and T_d is derivation time

Several research of PID, hybrid controller [26], and hybrid PID controllers [27]–[30] have been conducted until now that indicated better performance than other types of controllers such as fuzzy controllers [31]. Meanwhile, a hybrid controller such as fuzzy-PID has the benefit of having better system response [32], compared to the traditional PID, provides a lower initial control signal [33], and performs better than other controllers in terms of system robustness as well as parameter variation [34]. In situations when a traditional PID structure with constant coefficients may not perform, another type of PID, sigmoid PID delivers a faster controller response with less overshoot [35].

2.5. Hybrid PID and ILC

The PID feedback controls are ineffective for systems that have both continuous and discrete dynamics. We can use hybrid control for that situation [36]. For instance, we can use PID control combined with ILC. More than a decade of study has gone into ILC, and the work by Arimoto *et al.* [37] is widely cited as the primary source of motivation for research in this field [37]. As the name suggests, ILC is a recurrent process control technique. It is essential for applications exploring trajectory tracking control over a limited interval [0, T]. It concentrates on issues where interaction between passes is typically zero but where repetition of a single task allows for performance improvement from task to task [38]. Even in situations where repetitive tasks are done over fixed periods, ILC is an efficient method for improving transient response and tracking performance in the presence of parametric uncertainties and unmodeled dynamics [39], [40]. For a system that executes the same trajectory repeatedly, ILC is a relatively novel control method. Using this technique, we can enhance both transient responsiveness and tracking performance [41]. A modest PID gain should be used in most situations. Especially if the intrinsic frequency of the system is not properly evaluated, high PID gains might cause system vibrations. When the adjusted control signal reaches the intended trajectory, the ILC is utilized to fine-tune it.

There is considerable nonlinearity, strong coupling, and time-varying dynamic characteristics in the lower limb exoskeleton. The mathematical model employed to construct it is ambiguous and may cause system instability. For the most part, iterative learning control does not require any specific models. It is ideal for controlling objects which move in a finite period. The tracking error is modified according to the learning signal to enhance a particular control goal and track the intended trajectory [42], [43]. In brief, because the PID has strong robustness and the ILC has good performance, it is assumed that their combination will have both [44]. Figure 7 depicts a diagram block of hybrid PID-ILC applied to the exoskeleton, where u_j is ILC control signal, k_p is proportional value, k_d is derivative value, k_i is integral value, e_j is error between desired and actual outputs (y_d to y_j), and j is number of iterations
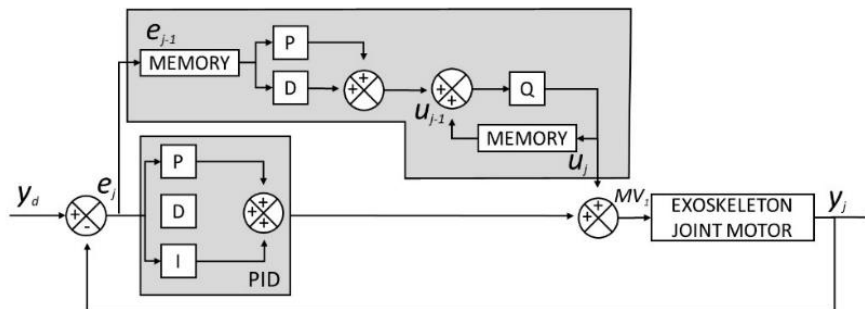

Figure 7. Block diagram of Hybrid PID-ILC applied to an exoskeleton

2.6. Microcontroller and motor driving system

The wiring diagram of the microcontroller and motor driving system is shown in Figure 8. A 24 V lithium-ion battery is used to power the DC motor and electronic circuits of the exoskeleton. Then the switched regulators convert 24 volts DC from the battery to 5 volts to supply the electronic circuits. The gait trajectories are stored in the microcontroller's memory, an Atmel ATmega 328 on the Arduino platform. Each time the microcontroller will send the position data to motor drivers. The BTS7960 High current motor driver h-bridge module will amplify the currents so there will be enough current to drive the DC motors (PG56 DC motors). Each motor can drive a single joint. The encoder will send back the actual position of the joints as the inputs of the microcontroller. Then the microcontroller will compute the voltage value to be sent to driver circuits.
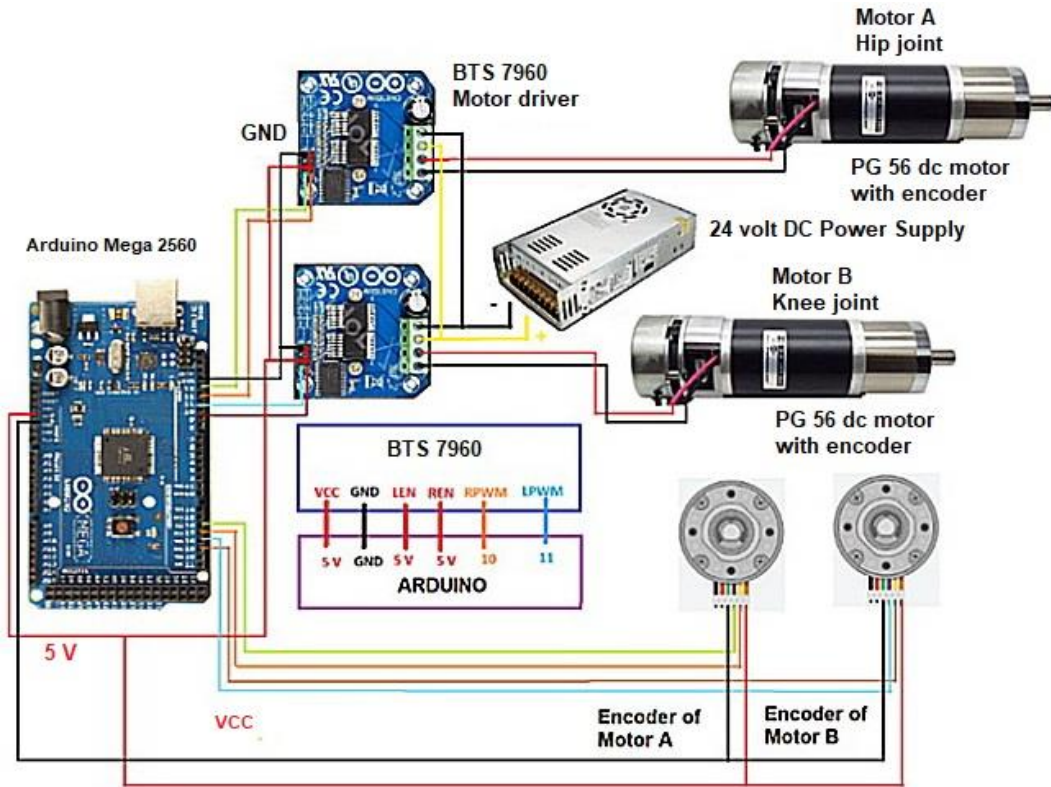
Figure 8. Wiring diagram of microcontroller and motor driving system

3. RESULTS AND DISCUSSION

In this work, a normal gait pattern used as the reference trajectory was provided by previous experiments dataset from healthy subjects [45]. Figures 9 and 10 respectively show the graphs of the flexion and extension movements of hip and knee joints based on that data. Figure 9 shows that the range of hip flexion/extension is from -18 to 25 degrees. While in Figure 10, the range of the knee flexion/extension is from 0 to 60 degrees.

The microcontroller executed data and transferred it to a driver to move the DC motor based on stored trajectory data by utilizing a control algorithm. There are two steps in applying the hybrid PID-ILC algorithm. Firstly, just use the PID control without ILC and make it stable by tuning the PID parameters, Kp, Ki, and Kd. Table 2 [46] can be used for reference for the PID tuning. After the PID response is stable, the ILC learning algorithm can be activated.
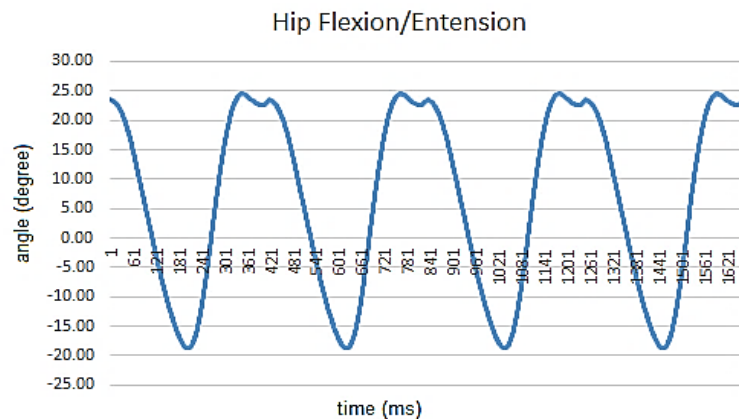

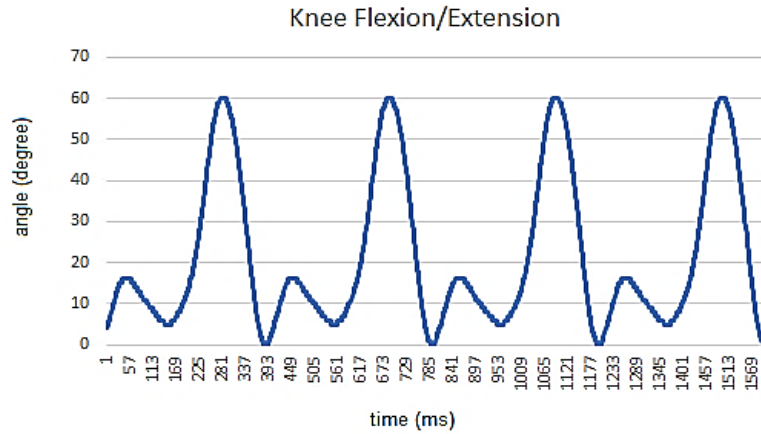Figure 9. Flexion and extension movements of hip based on the dataset

Figure 10. Flexion and extension movements of the knee based on the dataset

Table 2. PID controller tuning parameters

Response	Rise time	Overshoot	Settling time	S-S error
Kp	Decrease	Increase	Small Change	Decrease
Ki	Decrease	Increase	Increase	Decrease
Kd	Small Change	Decrease	Decrease	No Change

In Figures 11 to 14, we can observe the location of the hip and knee joints of the exoskeleton. As illustrated in Figures 11 and 13, PID only results in a significant steady-state error, yet the system remains stable. As shown in Figure 11, the PID-only controller is being used to control hip movement. The exoskeleton moved along with the load from the lower limb. The range of hip flexion/extension is -15 until 20 degrees. The system is stable, but there are steady-state errors between 0 to 10 degrees.

Figure 12 shows the hybrid PID-ILC controller being used to control the hip movement. Still, with the same controller gain and load, there are significant improvements in the performance in the initial move from 0 to 5 degrees. But after more than ten iterations, the steady-state errors can be minimized under 1 degree the range of hip just as the same with the set point.

In Figure 13, the PID-only controller is being used to control knee movement. The exoskeleton moved along with the same load from the lower limb and with the same controller gain. The range of knee flexion/extension is eight until 55 degrees. The system is also stable, but there are steady-state errors between 0 to 10 degrees.

In Figure 14, the hybrid PID-ILC controller is being used to control knee movement. Still, with the same controller gain and load, there are significant improvements in the performance in the initial move from 0 to 10 degrees. But after more than ten iterations, the steady-state errors can be minimized under 1 degree-the range of hip just as the same with the set point. Figures 12 and 14 show that it takes more than ten iterations to achieve the trajectory set point after using hybrid PID-ILC, as illustrated in Figures 12 and 14. The output filtering causes the phase difference. The output is sound, with a low steady-state error rate, according to the results.
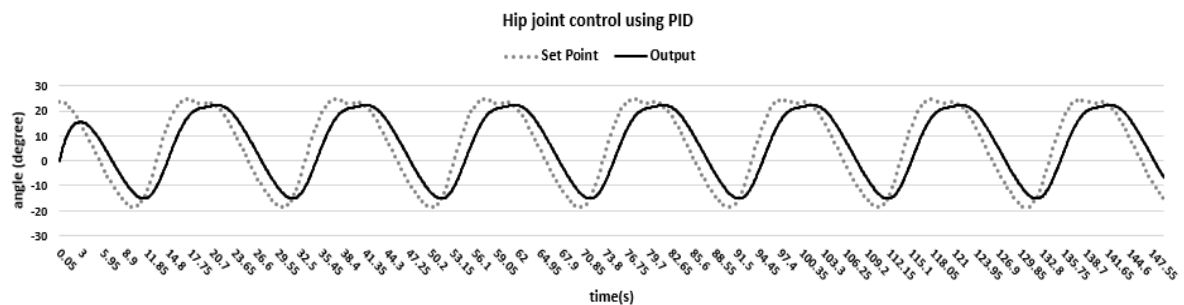

Figure 11. Flexion and extension movements of exoskeleton hip using PID only
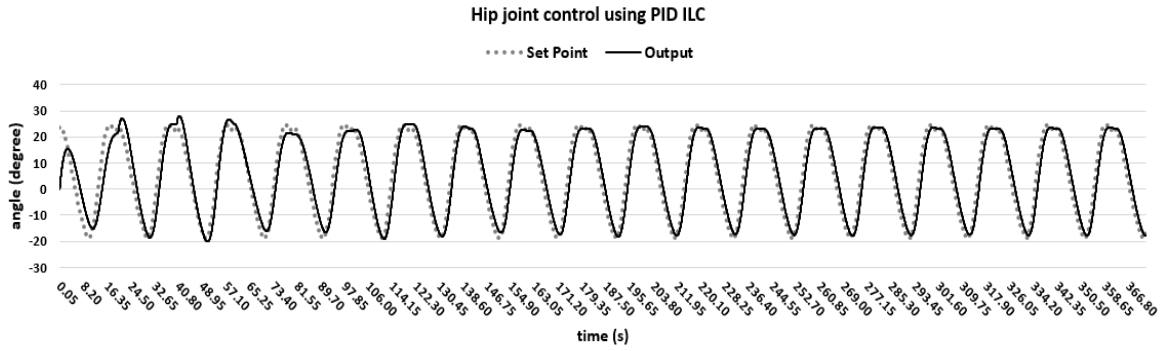
Hip joint control using PID ILC

········ Set Point ——— Output

Figure 12. Flexion and extension movements of exoskeleton hip using PID-ILC

Knee joint control using PID

········ Set Point ——— Output
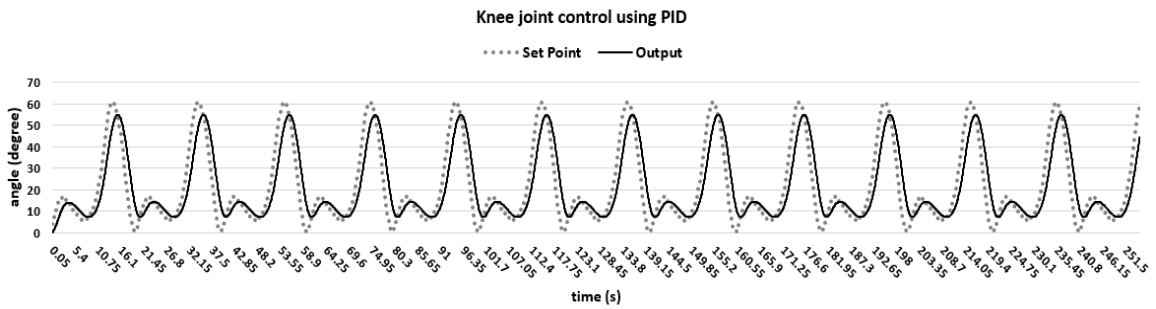
Figure 13. Flexion and extension movements of exoskeleton knee using PID only

Knee joint control using PID ILC
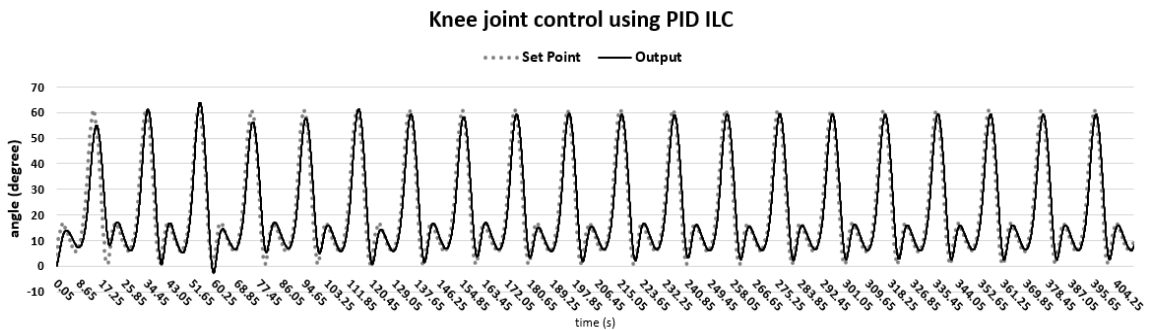
········ Set Point ——— Output

Figure 14. Flexion and extension movements of exoskeleton knee using PID-ILC

Assessment of system performance can be done by measuring or calculating the system's performance index. In this case, the mean square error (MSE) and the root mean square error (RMSE) can be used. The square RMSE is called MSE. The RMSE is a metric that compares the predicted values of a hypothetical model to the actual values [47]. Table 3 shows the numerical analysis comparison of PID and PID-ILC responses, based on the RMSE and MSE. It can be seen that steady-state errors are greatly reduced to 50%. Mean square error can be expressed as:

$$MSE = \frac{\sum_{j=1}^{V} E_j^2}{V}$$

where V is number of data. Root mean square error can be expressed as:

$$RMSE = \sqrt{\frac{\sum_{j=1}^{V} E_j^2}{V}}$$

Table 3. Numerical analysis comparison of PID and PID-ILC responses

Joints	Control type	RMSE	MSE
Hip	PID	0.141532	0.020031
	PID-ILC	0.080999698	0.01
Knee	PID	0.162832	0.026514
	PID-ILC	0.09	0.01

4. CONCLUSION

A gait trainer with a lower limb exoskeleton has been created. As a result of the suggested hybrid PID-ILC controller, a robot-assisted gait trainer with unmodeled dynamics, uncertainty, and disturbance can track the gait trajectory. The actual experiment using load and particular controller gain showed that the system controlled using PID only has stability but with steady-state errors up to 10 degrees. The proposed using hybrid PID-ILC controller showed stability with its initial steady-state error. But after more than ten iterations, the steady-state error can be reduced to less than 1 degree. The steady-state errors are greatly reduced to 50%.

ACKNOWLEDGEMENTS

REFERENCES

[1] Y. R. Li, *Cardiovascular diseases: from molecular pharmacology to evidence-based therapeutics*. New Jersey: John Wiley & Sons, 2015.
[2] E. J. Benjamin *et al.*, "Heart disease and stroke statistics—2017 Update: A report from the American heart association," *Circulation*, vol. 135, no. 10, Mar. 2017, doi: 10.1161/CIR.0000000000000485.
[3] N. Venketasubramanian, B. W. Yoon, J. Pandian, and J. C. Navarro, "Stroke epidemiology in South, East, and South-East Asia: A review," *Journal of Stroke*, vol. 19, no. 3, pp. 286–294, Sep. 2017, doi: 10.5853/jos.2017.00234.
[4] M. P. M. van Nunen, "Recovery of walking ability using a robotic device," *Amsterdam*, 2013. Accessed Jul. 06, 2021. [Online]. Available: https://research.vu.nl/files/42114296/complete dissertation.pdf
[5] K. H. Do and M. H. Chun, "Clinical use of robots as a part of rehabilitation medicine," *Brain & Neurorehabilitation*, vol. 10, no. 1, 2017, doi: 10.12786/bn.2017.10.e7.
[6] A. Esquenazi, "Comment on 'assessing effectiveness and costs in robot-mediated lower limbs rehabilitation: A meta-analysis and State of the art,'" *Journal of Healthcare Engineering*, vol. 2018, pp. 1–3, Nov. 2018, doi: 10.1155/2018/7634965.
[7] N. Radjou and J. Prabhu, *Frugal innovation: How to do better with less*. London: Profile Books, 2015.
[8] V.-T. Tran and P. Ravaud, "Frugal innovation in medicine for low resource settings," *BMC Medicine*, vol. 14, no. 1, Dec. 2016, doi: 10.1186/s12916-016-0651-1.
[9] Shiuh-Jer Huang and Ji-Shin Lee, "A stable self-organizing fuzzy controller for robotic motion control," *IEEE Transactions on Industrial Electronics*, vol. 47, no. 2, pp. 421–428, Apr. 2000, doi: 10.1109/41.836358.
[10] Byung Kook Yoo and Woon Chul Ham, "Adaptive control of robot manipulator using fuzzy compensator," *IEEE Transactions on Fuzzy Systems*, vol. 8, no. 2, pp. 186–199, Apr. 2000, doi: 10.1109/91.842152.
[11] D. A. Bristow, "A survey of iterative learning control," *IEEE Control Systems*, vol. 26, no. 3, pp. 96–114, Jun. 2006, doi: 10.1109/MCS.2006.1636313.
[12] D. A. Bristow, K. L. Barton, and A. G. Alleyne, *Iterative learning control*, Control Sy. Ed. Boca Raton: CRC Press, 2011.
[13] A. Madady, "PID type iterative learning control with optimal gains," *International Journal of Control, Automation, and Systems*, vol. 6, no. 2, pp. 194–203, 2008.
[14] A. P. P. A. Majeed *et al.*, "The control of a lower limb exoskeleton for gait rehabilitation: A hybrid active fForce control approach," *Procedia Computer Science*, vol. 105, pp. 183–190, 2017, doi: 10.1016/j.procs.2017.01.204.
[15] M. S. Amiri, R. Ramli, and M. F. Ibrahim, "Initialized model reference adaptive control for lower limb exoskeleton," *IEEE Access*, vol. 7, pp. 167210–167220, 2019, doi: 10.1109/ACCESS.2019.2954110.
[16] M. R. Tucker *et al.*, "Control strategies for active lower extremity prosthetics and orthotics: a review," *Journal of NeuroEngineering and Rehabilitation*, vol. 12, no. 1, p. 1, 2015, doi: 10.1186/1743-0003-12-1.
[17] D. Maneetham, *Industrial robotics & mechatronics applications*. Bangkok: SE-Education, 2018.
[18] J. Hamill, K. M. Knutzen, and T. R. Derrick, *Biomechanical basis of human movement*, 4th ed. Philadelphia: Lippincott Williams & Wilkins, 2015.
[19] K. H. Low, "Robot-assisted gait rehabilitation: From exoskeletons to gait systems," in *2011 Defense Science Research Conference and Expo (DSR)*, Aug. 2011, pp. 1–10, doi: 10.1109/DSR.2011.6026886.
[20] J. C. Moreno, F. Brunetti, E. Rocon, and J. L. Pons, "Immediate effects of a controllable knee ankle foot orthosis for functional compensation of gait in patients with proximal leg weakness," *Medical & Biological Engineering & Computing*, vol. 46, no. 1, pp. 43–53, Jan. 2008, doi: 10.1007/s11517-007-0267-x.
[21] J. M. Hollerbach, I. W. Hunter, and J. Ballantyne, *A comparative analysis of actuator technologies for robotics*. Cambridge: The MIT Press, 1992.
[22] J. G. Ziegler and N. B. Nichols, "Optimum settings for automatic controllers," *Journal of Dynamic Systems, Measurement, and Control*, vol. 115, no. 2B, pp. 220–222, Jun. 1993, doi: 10.1115/1.2899060.
[23] K. H. Ang, G. Chong, and Yun Li, "PID control system analysis, design, and technology," *IEEE Transactions on Control Systems*

Technology, vol. 13, no. 4, pp. 559–576, Jul. 2005, doi: 10.1109/TCST.2005.847331.

[24] K. J. Åström, T. Hägglund, C. C. Hang, and W. K. Ho, "Automatic tuning and adaptation for PID controllers - a survey," *Control Engineering Practice*, vol. 1, no. 4, pp. 699–714, Aug. 1993, doi: 10.1016/0967-0661(93)91394-C.

[25] O. A. Somefun, K. Akingbade, and F. Dahunsi, "The dilemma of PID tuning," *Annual Reviews in Control*, vol. 52, pp. 65–74, 2021, doi: 10.1016/j.arcontrol.2021.05.002.

[26] P. Sutyasadi and M. Parnichkun, "Push recovery control of quadruped robot using particle swarm optimization based structure specified mixed sensitivity $H_2/H\infty$ control," *Industrial Robot: the international journal of robotics research and application*, vol. 47, no. 3, pp. 423–434, Mar. 2020, doi: 10.1108/IR-06-2019-0135.

[27] M. W. Hasan and N. H. Abbas, "An improved swarm intelligence algorithms-based nonlinear fractional order-PID controller for a trajectory tracking of underwater vehicles," *TELKOMNIKA (Telecommunication Computing Electronics and Control)*, vol. 18, no. 6, pp. 3173–3183, Dec. 2020, doi: 10.12928/telkomnika.v18i6.16282.

[28] M. A. Faraj and A. Mohammed Abbood, "Fractional order PID controller tuned by bat algorithm for robot trajectory control," *Indonesian Journal of Electrical Engineering and Computer Science*, vol. 21, no. 1, pp. 74–83, Jan. 2021, doi: 10.11591/ijeecs.v21.i1.pp74-83.

[29] K. G. Abdulhussein, N. M. Yasin, and I. J. Hasan, "Comparison between butterfly optimization algorithm and particle swarm optimization for tuning cascade PID control system of PMDC motor," *International Journal of Power Electronics and Drive Systems (IJPEDS)*, vol. 12, no. 2, pp. 736–744, Jun. 2021, doi: 10.11591/ijpeds.v12.i2.pp736-744.

[30] J. A. Shah and S. S. Rattan, "Dynamic analysis of two link robot manipulator for control design using PID computed torque control.," *IAES International Journal of Robotics and Automation (IJRA)*, vol. 5, no. 4, pp. 277–283, Dec. 2016, doi: 10.11591/ijra.v5i4.pp277-283.

[31] A. Prayitno, V. Indrawati, and I. Trusulaw, "International conference on recent trends in physics 2016 (ICRTP2016)," *Journal of Physics: Conference Series*, vol. 755, Oct. 2016, doi: 10.1088/1742-6596/755/1/011001.

[32] I. Erenoglu, I. Eksin, E. Yesil, and M. Guzelkaya, "An intelligent hybrid fuzzy Pid controller," in *ECMS 2006 Proceedings edited by: W. Borutzky, A. Orsoni, R. Zobel*, May 2006, pp. 62–66, doi: 10.7148/2006-0062.

[33] K. Abidi and J.-X. Xu, *Advanced discrete-time control*, vol. 23. Singapore: Springer Singapore, 2015.

[34] D. Somwanshi, M. Bundele, G. Kumar, and G. Parashar, "Comparison of fuzzy-PID and PID controller for speed control of DC motor using LabVIEW," *Procedia Computer Science*, vol. 152, pp. 252–260, 2019, doi: 10.1016/j.procs.2019.05.019.

[35] N. H. Abdul Razak Ramesh, M. R. Ghazali, and M. A. Ahmad, "Sigmoid PID based adaptive safe experimentation dynamics algorithm of portable duodopa pump for Parkinson's disease patients," *Bulletin of Electrical Engineering and Informatics*, vol. 10, no. 2, pp. 632–639, Apr. 2021, doi: 10.11591/eei.v10i2.2542.

[36] R. G. Sanfelice, *Hybrid feedback control*. Princeton: Princeton University Press, 2021.

[37] S. Arimoto, S. Kawamura, and F. Miyazaki, "Bettering operation of robots by learning," *Journal of Robotic Systems*, vol. 1, no. 2, pp. 123–140, 1984, doi: 10.1002/rob.4620010203.

[38] D. H. Owens and J. Hätönen, "Iterative learning control — An optimization paradigm," *Annual Reviews in Control*, vol. 29, no. 1, pp. 57–70, Jan. 2005, doi: 10.1016/j.arcontrol.2005.01.003.

[39] F.-M. Chen *et al.*, "An improvement on the transient response of tracking for the sampled-data system based on an improved PD-type iterative learning control," *Journal of the Franklin Institute*, vol. 351, no. 2, pp. 1130–1150, Feb. 2014, doi: 10.1016/j.jfranklin.2013.10.014.

[40] X. Li, Q. Ren, and J. Xu, "Precise speed tracking control of a robotic fish via iterative learning control," *IEEE Transactions on Industrial Electronics*, vol. 63, no. 4, pp. 1–1, 2015, doi: 10.1109/TIE.2015.2499719.

[41] K. L. Moore, *Iterative learning control for deterministic systems*. London: Springer London, 1993.

[42] P. Sutyasadi and M. Parnichun, "Trotting control of a quadruped robot using PID-ILC," in *IECON 2015 - 41st Annual Conference of the IEEE Industrial Electronics Society*, Nov. 2015, pp. 4400–4405, doi: 10.1109/IECON.2015.7392784.

[43] D. Maneetham and P. Sutyasadi, "Controlling a knee CPM machine using PID and iterative learning control algorithm," *TELKOMNIKA (Telecommunication Computing Electronics and Control)*, vol. 18, no. 2, pp. 1047–1053, Apr. 2020, doi: 10.12928/telkomnika.v18i2.14876.

[44] M. Rezaei Estakhrouieh and A. Gharaveisi, "Optimal iterative learning control design for generator voltage regulation system," *Turkish Journal of Electrical Engineering and Computer Sciences*, vol. 21, pp. 1909–1919, 2013, doi: 10.3906/elk-1203-19.

[45] G. Bovi, M. Rabuffetti, P. Mazzoleni, and M. Ferrarin, "A multiple-task gait analysis approach: Kinematic, kinetic and EMG reference data for healthy young and adult subjects," *Gait & Posture*, vol. 33, no. 1, pp. 6–13, Jan. 2011, doi: 10.1016/j.gaitpost.2010.08.009.

[46] P. O. J. Kaltjob, Control of mechatronic systems: model-driven design and implementation guidelines. West Sussex: John Wiley & Sons, 2021.

[47] N. J. Salkind, B. B. Frey, D. M. Dougherty, K. R. Teasdale, and N. Hill-Kapturczak, *Encyclopedia of research design*. Thousand Oaks, California: SAGE Publications, 2010.

BIOGRAPHIES OF AUTHORS

Elang Parikesit 🆔 🔷 🆂🅲 ◐ received his bachelor's degree in electrical engineering from Diponegoro University, Indonesia in 1997 and a master's degree in biomedical engineering from Institut Teknologi Bandung (ITB) in 2012. He is a lecturer at the Electromedical Technology Department of Sanata Dharma University, Yogyakarta, Indonesia. He went to Rajamangala University of Technology Thanyaburi, Thailand to continue his doctoral degree in mechatronics engineering. His research interest includes renewable energy, mechatronics, and biomedical engineering. He can be contacted at email: elang_p@mail.rmutt.ac.th or elang@usd.ac.id.

Dechrit Maneetham ⬤ 🔗 SC ↻ is an Associate Professor of Mechatronics Engineering at Rajamangala University of Technology Thanyaburi, Thailand. He received his B.Tech. and M.S. degrees from King Mongkut's University of Technology, North Bangkok and his D.Eng. in Mechatronics degree from the Asian Institute of Technology in 2010, and his Ph.D. in Electrical and Computer Engineering from Mahasarakham University in 2018. His research interest includes biomedical applications, robotics and automation applications, and mechatronics applications. He can be contacted at email: dechrit_m@rmutt.ac.th.

Petrus Sutyasadi ⬤ 🔗 SC ↻ obtained a master's degree in mechatronics in 2008 and a doctorate in mechatronics in 2016 from the Asian Institute of Technology in Thailand. Currently. He is a lecturer at the Department of Mechatronics Engineering, Sanata Dharma University, Yogyakarta, Indonesia. His research interests include robust control, robotics, and frugal innovation in mechatronic engineering. He can be contacted at email: peter@usd.ac.id.